NCAR Manuscript No. 139

The influence of compensating downward motion on the development of cumulus clouds*

by

Tomio Asai** and Akira Kasahara

National Center for Atmospheric Research

Boulder, Colorado

February 1966

---

*A part of this paper was presented at the Fourth Technical Conference on Hurricanes and Tropical Meteorology, Miami, Florida, November 1965.

**On leave from the Meteorological Research Institute, Japan Meteorological Agency.

Abstract

An attempt is made to assess the effects of the compensating downward motion associated with the updraft upon the development of a cumulus cloud. The model consists of two circular concentric air columns: the inside column (core) corresponds to the updraft region (cloud area) and the outside concentric annular column corresponds to the downward motion region (cloudless area). The combined cell is surrounded by the atmosphere at rest. The governing equations of both the updraft and the compensating downward motion are derived from the conservation equations of momentum, heat, moisture and mass.

The set of differential equations is solved numerically to show how the vertical velocity, temperature, specific humidity and liquid water content in and out of the cloud area will change with height and time, and to examine the effect of the downward motion upon the development of the cloud. The main results are the following: When the environmental atmosphere is relatively dry and without a steady source of moisture, tall clouds never develop. The compensating downward motion seems to have little influence on the evolution of the cloud in this case. When the environmental atmosphere is relatively moist, the structure of the single column updraft tends to a steady state, if we neglect the effect of the compensating downward motion. However, with the compensating downward motion, no tall cloud is maintained unless there is a steady source of moisture at the cloud base. It is apparent that the compensating downward motion acts as a "break" which prevents the maintenance of a tall cumulus cloud.

1. Introduction

In order to explain differences between observations made in cumulus clouds and the theory of adiabatic parcel ascent, Stommel (1947) introduced an idea of "entrainment". The basic premise is that the ascending current in the clouds entrains air from their surroundings. The entrained air modifies the mechanical and thermodynamic characteristics of the ascending current. Based upon the concept of "entrainment" many studies of cumulus convection were developed by Austin and Fleisher (1948), Byers and Braham (1949), Houghton and Cramer (1951), Bunker (1953) and others.

Two different views have been presented on the physical mechanisms of entrainment. Stommel (1947) visualized entrainment caused by turbulent lateral mixing in a manner which has been discussed in the jet-stream theories. On the other hand, Austin (1948) took a view that entrainment is necessary to satisfy the mass continuity in the vertical stretching of an accelerated convective column. According to Houghton and Cramer (1951), this particular type of entrainment is called "dynamic entrainment". For convenience, we shall call the former type "jet entrainment". It is our view that the amount of "jet entrainment" is the sum of the amount of "dynamic entrainment" and of that entrainment which is due entirely to a turbulent eddy exchange mechanism. The same viewpoint has been taken by Haltiner (1959), Mason and Emig (1961) and Asai (1962). In their models of cumulus clouds, it is assumed that the cross section area of the cloud is independent of height. This assumption was discarded in the work of Squires and Turner (1962), and the shape of the cloud was computed.

An alternative to the idea of a continuous updraft modified by entrainment was proposed by Scorer and Ludlam (1953). In their context, the updraft in a cumulus cloud consists of a succession of thermals or bubbles. The theoretical development by Levine (1959), however, shows that the form of the equation for the vertical velocity of the bubble's center of mass is identical to the equation of vertical motion in the jet models. The exception is that in the bubble theory the effect of aerodynamic drag is inversely proportional to the diameter of the bubble, whereas in the jet model, the effect of entrainment is inversely proportional to the diameter of the jet itself.

It is apparent that the previous studies of cumulus clouds were concerned primarily with the physical forms of buoyant elements in the updraft and the mechanism of entrainment of environmental air into the updraft. In all of these studies, the cloud consists of only a single updraft in an environment at rest and no consideration is made of the effect of compensating downward currents associated with the updraft. From observations of cumulonimbus clouds and of Bénard cell convections, it is evident that the role of compensating currents is important. It is well known that the development of moist adiabatic ascending motions is suppressed in an environment with dry-adiabatic downward motions. It was shown by J. Bjerknes (1938) that cumulus convections do not occur unless the ratio between the width of the cumulus towers and that of the cloudless intervals is below a certain critical value. In this paper, an attempt will be made to extend the Bjerknes theory by including the effect of entrainment in the updraft.

Our model consists of two concentric air columns: the inside column corresponds to an updraft region (cloud area) and the outside concentric annular column corresponds to a downward motion region (cloudless area). The geometric configuration of the model is illustrated in Fig. 1.

Fig. 1

Circular symmetric cells adopted here are regarded as approximations of equilateral hexagons. The radii of the inside and outside columns are denoted by "a" and "b" respectively. The ratio σ defined by

$$\sigma = a/b \tag{1.1}$$

is going to be an important parameter in this study. Thus, σ^2 represents the ratio of the area of updraft to that of the whole system. Hereafter, σ^2 will be referred to as the "area density of the updraft".

Interactions between the inside and the outside columns are considered through the buoyant force which depends on the temperature difference between the air in the ascending area and the air in the descending area. We also consider the dynamic entrainment and the turbulent mixing through the lateral boundary between the ascending and descending cells.

2. Basic equations

We consider radial-vertical motions in the cylindrical coordinates (r, λ, z), where r, λ, and z denote the radial, tangential and height

coordinates. The vertical component of the equation of motion is written as

$$\frac{\partial w}{\partial t} + u\frac{\partial w}{\partial r} + w\frac{\partial w}{\partial z} = -\frac{1}{\rho}\frac{\partial p}{\partial z} - g \tag{2.1}$$

where w and u are the vertical (positive upwards) and radial (positive outwards) components of the velocity; p denotes the pressure; ρ, the density of air and g the acceleration due to gravity.

We assume that the equation of mass continuity can be approximated by

$$\frac{1}{r}\frac{\partial}{\partial r}(\rho_o r u) + \frac{\partial}{\partial z}(\rho_o w) = 0 \tag{2.2}$$

where ρ_o denotes a mean density defined by the hydrostatic equation

$$\frac{\partial p_o}{\partial z} = -\rho_o g \tag{2.3}$$

where p_o denotes a horizontally averaged pressure.

It is convenient to introduce here the potential temperature θ and the virtual potential temperature θ_v defined by

$$\theta = T\left(\frac{p_s}{p}\right)^{\varkappa} \quad ; \qquad \varkappa = R/C_p \tag{2.4}$$

and

$$\theta_v = (1 + 0.608q)\ \theta \tag{2.5}$$

where T denotes the temperature; C_p, the specific heat of dry air at constant pressure; R, the gas constant for dry air; q, the specific humidity; p_s represents 1000 mb.

With the aid of (2.2), Eq. (2.1) may be written in the following form

$$\rho_o \frac{\partial w}{\partial t} + \frac{1}{r}\frac{\partial}{\partial r}(\rho_o r w u) + \frac{\partial}{\partial z}(\rho_o w w) = \rho_o\left(\frac{\theta_v - \theta_{vo}}{\Theta}\right) g \tag{2.6}$$

where θ_{vo} represents a horizontally averaged value of θ_v and Θ denotes a vertically averaged value of θ_{vo}. In order to derive Eq. (2.6), it was assumed that the pressure p adjusts instantaneously to that of the mean pressure p_o, so that the deviation from the hydrostatic equilibrium given on the right-hand side of (2.1) is expressed only by the buoyancy as adopted customarily in the jet models of convection (Morton, Taylor and Turner, 1956).

We use the thermodynamic equation written in the form

$$\rho_o \frac{\partial \theta}{\partial t} + \frac{1}{r}\frac{\partial}{\partial r}(\rho_o r \theta u) + \frac{\partial}{\partial z}(\rho_o \theta w) = \frac{L}{C_p}\left(\frac{P_s}{p_o}\right)^{\kappa} \rho_o M \tag{2.7}$$

where L denotes the latent heat of condensation and M represents the rate of condensation of water vapor. The same method described by Asai (1965) is used in this study to compute the rate of condensation.

The equations of continuity for water vapor and liquid water may be written, respectively, as

$$\rho_o \frac{\partial q}{\partial t} + \frac{1}{r}\frac{\partial}{\partial r}(r\rho_o qu) + \frac{\partial}{\partial z}(\rho_o qw) = -\rho_o M , \tag{2.8}$$

$$\rho_o \frac{\partial m}{\partial t} + \frac{1}{r}\frac{\partial}{\partial r}(r\rho_o mu) + \frac{\partial}{\partial z}(\rho_o mw) = \rho_o M \tag{2.9}$$

where q and m are the specific humidity and the liquid water content, respectively.

The five equations (2.2), (2.6), (2.7), (2.8) and (2.9) form a system of equations governing the five dependent variables u, w, θ, q and m.

3. Horizontal averaging of the basic equations

In order to derive the system of equations for the variables averaged over the inner area, we integrate Eqs. (2.6), (2.7), (2.8), (2.9) and (2.2) over the cross section of the inner column and then, dividing the resulting equations by $\rho_o \pi a^2$, we obtain the following set of equations

$$\frac{\partial \bar{w}_a}{\partial t} + \frac{2}{a}\left(\tilde{\bar{w}}_a \tilde{\bar{u}}_a + \widetilde{w_a'' u_a''}\right) + \frac{1}{\rho_o}\frac{\partial}{\partial z}\left[\rho_o\left(\bar{\bar{w}}_a \bar{\bar{w}}_a + \overline{w_a' w_a'}\right)\right]$$

$$= \left(\frac{\bar{\theta}_{va} - \theta_{vo}}{\Theta}\right) g \quad , \tag{3.1}$$

$$\frac{\partial \bar{\theta}_a}{\partial t} + \frac{2}{a}\left(\tilde{\bar{\theta}}_a \tilde{\bar{u}}_a + \widetilde{\theta_a'' u_a''}\right) + \frac{1}{\rho_o}\frac{\partial}{\partial z}\left[\rho_o\left(\bar{\bar{\theta}}_a \bar{\bar{w}}_a + \overline{\theta_a' w_a'}\right)\right]$$

$$= \frac{L}{C_p}\left(\frac{p_s}{p_o}\right)^{\varkappa} \bar{M}_a \quad , \tag{3.2}$$

$$\frac{\partial \bar{q}_a}{\partial t} + \frac{2}{a}\left(\tilde{q}_a \tilde{u}_a + \widetilde{q_a'' u_a''}\right) + \frac{1}{\rho_o}\frac{\partial}{\partial z}\left[\rho_o\left(\bar{q}_a \bar{w}_a + \overline{q_a' w_a'}\right)\right]$$

$$= -\bar{M}_a \quad , \tag{3.3}$$

$$\frac{\partial \bar{m}_a}{\partial t} + \frac{2}{a}\left(\tilde{m}_a \tilde{u}_a + \widetilde{m_a'' u_a''}\right) + \frac{1}{\rho_o}\frac{\partial}{\partial z}\left[\rho_o\left(\bar{m}_a \bar{w}_a + \overline{m_a' w_a'}\right)\right]$$

$$= \bar{M}_a \quad , \tag{3.4}$$

$$\frac{2}{a}\,\tilde{u}_a + \frac{1}{\rho_o}\frac{\partial}{\partial z}(\rho_o \bar{w}_a) = 0. \tag{3.5}$$

Here we used the following notations for any variable A.

$$\bar{A}_a \equiv \frac{1}{\pi a^2}\int_0^{2\pi}\int_0^a A\, r\, dr\, d\lambda \quad ,$$

$$\tilde{A}_a \equiv \frac{1}{2\pi}\int_0^{2\pi} A\, d\lambda \quad \text{at } r = a,$$

$$A_a' = A - \bar{A}_a \quad , \quad A_a'' = A - \tilde{A}_a \quad . \tag{3.6}$$

Similarly, we integrate Eqs. (2.6), (2.7), (2.8), (2.9), and (2.2) over the cross section of the outer annular column, and dividing the resulting equations by $\rho_o \pi (b^2 - a^2)$, we obtain

$$\frac{\partial \bar{w}_b}{\partial t} + \frac{2}{b^2 - a^2}\left[b(\tilde{w}_b \tilde{u}_b + \widetilde{w_b'' u_b''}) - a(\tilde{w}_a \tilde{u}_a + \widetilde{w_a'' u_a''})\right]$$

$$+ \frac{1}{\rho_o}\frac{\partial}{\partial z}\left[\rho_o\left(\bar{w}_b \bar{w}_b + \overline{w_b' w_b'}\right)\right] = \left(\frac{\bar{\theta}_{vb} - \theta_{vo}}{\Theta}\right) g \quad , \tag{3.7}$$

$$\frac{\partial \bar{\theta}_b}{\partial t} + \frac{2}{b^2-a^2}\left[b\left(\tilde{\theta}_b\tilde{u}_b + \widetilde{\theta_b''u_b''}\right) - a\left(\tilde{\theta}_a\tilde{u}_a + \widetilde{\theta_a''u_a''}\right)\right]$$

$$+ \frac{1}{\rho_o}\frac{\partial}{\partial z}\left[\rho_o\left(\bar{\theta}_b\bar{w}_b + \overline{\theta_b'w_b'}\right)\right] = \frac{L}{C_p}\left(\frac{p_s}{p_o}\right)^{\kappa}\bar{M}_b \quad , \tag{3.8}$$

$$\frac{\partial \bar{q}_b}{\partial t} + \frac{2}{b^2-a^2}\left[b\left(\tilde{q}_b\tilde{u}_b + \widetilde{q_b''u_b''}\right) - a\left(\tilde{q}_a\tilde{u}_a + \widetilde{q_a''u_a''}\right)\right]$$

$$+ \frac{1}{\rho_o}\frac{\partial}{\partial z}\left[\rho_o\left(\bar{q}_b\bar{w}_b + \overline{q_b'w_b'}\right)\right] = -\bar{M}_b \quad , \tag{3.9}$$

$$\frac{\partial \bar{m}_b}{\partial t} + \frac{2}{b^2-a^2}\left[b\left(\tilde{m}_b\tilde{u}_b + \widetilde{m_b''u_b''}\right) - a\left(\tilde{m}_a\tilde{u}_a + \widetilde{m_a''u_a''}\right)\right]$$

$$+ \frac{1}{\rho_o}\frac{\partial}{\partial z}\left[\rho_o\left(\bar{m}_b\bar{w}_b + \overline{m_b'w_b'}\right)\right] = \bar{M}_b \quad , \tag{3.10}$$

$$\frac{2}{b^2-a^2}\left(b\,\tilde{u}_b - a\,\tilde{u}_a\right) + \frac{1}{\rho_o}\frac{\partial}{\partial z}\left(\rho_o\bar{w}_b\right) = 0 \quad , \tag{3.11}$$

where, for any variable A,

$$\bar{A}_b \equiv \frac{1}{\pi(b^2-a^2)} \int_0^{2\pi} \int_a^b A\, r\, dr d\lambda \,,$$

$$\tilde{A}_b \equiv \frac{1}{2\pi} \int_0^{2\pi} A\, d\lambda \quad \text{at } r = b,$$

$$A_b' = A - \bar{A}_b \,; \qquad A_b'' = A - \tilde{A}_b \,. \tag{3.12}$$

In Eqs. (3.1) to (3.4), and (3.7) to (3.10), there are terms such as $\widetilde{A_a''u_a''}$, $\widetilde{A_b''u_b''}$, $\overline{A_a'w_a'}$ and $\overline{A_b'w_b'}$ where A stands for one of the variables w, θ, q and m. The first two terms represent the <u>lateral</u> eddy fluxes of vertical momentum, heat, water vapor and liquid water through the cell boundaries located respectively at radii a and b. The last two terms represent the <u>vertical</u> eddy fluxes of the above mentioned transport quantities in the inner and outer areas respectively. As discussed in the Introduction, the <u>lateral</u> eddy exchanges of momentum, heat, etc., between the updraft of a cumulus cloud and its relatively quiet surrounding air are very important from the standpoint of entrainment. Therefore, in this study, we will take into account only the effect of $\widetilde{A_a''u_a''}$ term and neglect the terms

$\widetilde{A_b''u_b''}$, $\overline{A_a'w_a'}$ and $\overline{A_b'w_b'}$. Applying the exchange hypothesis, we assume that

$$\widetilde{A_a''u_a''} = -\frac{\nu}{a}(\bar{A}_b - \bar{A}_a) \tag{3.13}$$

where ν denotes the kinematic eddy exchange coefficient. For simplicity, the value of ν is assumed to be the same for all the transport quantities, w, θ, q and m.

By integrating (2.2) over the circular area of radius b and dividing the result by $\rho_o \pi b^2$, we obtain

$$2\frac{\tilde{u}_b}{b} + \frac{1}{\rho_o}\frac{\partial}{\partial z}(\rho_o w_o) = 0 \tag{3.14}$$

where

$$w_o \equiv \frac{1}{\pi b^2}\int_0^{2\pi}\int_0^b w\, r\, dr d\lambda . \tag{3.15}$$

From (3.11) we eliminate $\tilde{u}_a$ by using (3.5) and $\tilde{u}_b$ by using (3.14). The result is

$$\frac{\partial}{\partial z}\rho_o\left[\sigma^2\bar{w}_a + (1-\sigma^2)\bar{w}_b - w_o\right] = 0$$

where the definition of σ is given by (1.1).

By applying the boundary conditions that $\bar{w}_a = \bar{w}_b = w_o = 0$ at $z = 0$, we obtain

$$\sigma^2 \bar{w}_a + (1 - \sigma^2)\bar{w}_b = w_o . \tag{3.16}$$

To simplify the model, we assume that

$$w_o = 0. \tag{3.17}$$

Namely, the mean vertical velocity over the cross section of the model vanishes. This condition leads to

$$\tilde{u}_b = 0 \tag{3.18}$$

from (3.14). With the use of condition (3.17), it is clear from (3.16) that we need only one time dependent equation for either $\bar{w}_a$ or $\bar{w}_b$.

With the aid of (3.13), (3.17), (3.18), (3.5) and (3.11), we can rewrite Eqs. (3.1) to (3.5) and (3.7) to (3.11) as follows:

$$\frac{\partial w_a}{\partial t} = - w_a \frac{\partial w_a}{\partial z} + \frac{2}{b\sigma} (w_a - \tilde{w}_a)\, \tilde{u}_a$$

$$+ \frac{2\nu}{b^2 a^2} (w_b - w_a) + g \left(\frac{\theta_{va} - \theta_{vo}}{\theta} \right) , \tag{3.19}$$

$$\frac{\partial \theta_a}{\partial t} = - w_a \frac{\partial \theta_a}{\partial z} + \frac{2}{b\sigma} (\theta_a - \tilde{\theta}_a) \tilde{u}_a$$

$$+ \frac{2\nu}{b^2\sigma^2} (\theta_b - \theta_a) + \frac{L}{C_p} \left(\frac{p_s}{p_o} \right)^{\varkappa} M_a \, , \tag{3.20}$$

$$\frac{\partial q_a}{\partial t} = - w_a \frac{\partial q_a}{\partial z} + \frac{2}{b\sigma} (q_a - \tilde{q}_a) \tilde{u}_a$$

$$+ \frac{2\nu}{b^2\sigma^2} (q_b - q_a) - M_a \, , \tag{3.21}$$

$$\frac{\partial m_a}{\partial t} = - w_a \frac{\partial m_a}{\partial z} + \frac{2}{b\sigma} (m_a - \tilde{m}_a) \tilde{u}_a$$

$$+ \frac{2\nu}{b^2\sigma^2} (m_b - m_a) + M_a \, , \tag{3.22}$$

$$\frac{2}{b\sigma} \tilde{u}_a + \frac{1}{\rho_o} \frac{\partial}{\partial z} (\rho_o w_a) = 0 \, , \tag{3.23}$$

$$\frac{\partial \theta_b}{\partial t} = -w_b \frac{\partial \theta_b}{\partial z} - \frac{2\sigma}{b(1-\sigma^2)} (\theta_b - \tilde{\theta}_a) \tilde{u}_a$$

$$- \frac{2\nu}{b^2(1-\sigma^2)} (\theta_b - \theta_a) + \frac{L}{C_p} \left(\frac{p_s}{p_o}\right)^{\kappa} M_b \ , \qquad (3.24)$$

$$\frac{\partial q_b}{\partial t} = - w_b \frac{\partial q_b}{\partial z} - \frac{2\sigma}{b(1-\sigma^2)} (q_b - \tilde{q}_a) \tilde{u}_a$$

$$- \frac{2\nu}{b^2(1-\sigma^2)} (q_b - q_a) - M_b \ , \qquad (3.25)$$

$$\frac{\partial m_b}{\partial t} = - w_b \frac{\partial m_b}{\partial z} - \frac{2\sigma}{b(1-\sigma^2)} (m_b - \tilde{m}_a) \tilde{u}_a$$

$$- \frac{2\nu}{b^2(1-\sigma^2)} (m_b - m_a) + M_b \ , \qquad (3.26)$$

$$\sigma^2 w_a + (1-\sigma^2) w_b = 0 \ . \qquad (3.27)$$

The quantity θ_{vo} in (3.19) is, as mentioned earlier, the horizontally averaged value of θ_v given by

$$\theta_{vo} = \frac{1}{\pi b^2} \int_0^{2\pi} \int_0^b \theta_v \, r \, dr d\lambda$$

$$= \sigma^2 \, \theta_{va} + (1 - \sigma^2) \, \theta_{vb} \, . \qquad (3.28)$$

Note that in Eqs. (3.19) to (3.28), we omitted bar symbols over the variables which were defined in (3.6) and (3.12).

In Eqs. (3.19) to (3.27), the following four quantities $\tilde{w}_a$, $\tilde{\theta}_a$, $\tilde{q}_a$ and $\tilde{m}_a$ are still unspecified. Following a similar procedure discussed by Asai (1962), it is assumed that

$$\tilde{A}_a = A_a \qquad \text{if} \quad \tilde{u}_a > 0 \, ,$$

$$\tilde{A}_a = A_b \qquad \text{if} \quad \tilde{u}_a < 0 \, . \qquad (3.29)$$

This means that if there is a net inflow into the inner column and the entrained air transports A_b into the inner area, the mixing of the entrained air with the air in the inner column contributes to the local time change of A_a by the amount of $\frac{2}{\sigma b} (A_a - A_b) \tilde{u}_a$. Similarly, if there is a net outflow in the inner column and the air transports A_a out to the outer

area, the mixing of the detrained air with the air in the outer cell contributes to the local time change of A_b by the amount of

$\frac{2\sigma}{b(1 - \sigma^2)} (A_a - A_b) \tilde{u}_a$. This kind of entrainment or detrainment is called the dynamic entrainment after Houghton and Cramer (1951) and is required to satisfy the mass continuity between the inner and outer cells.

The third terms on the right-hand side of Eqs. (3.19) to (3.22) and (3.24) to (3.26) represent the lateral turbulent exchanges of momentum, heat, water vapor and liquid water, respectively. Following Richardson's empirical rule (1926), we assume

$$\nu = 0.6\, a^{4/3} \tag{3.30}$$

where a is the radius of the inner column in units of cm and ν is the exchange coefficient in units of $cm^2\ sec^{-1}$.

The fourth term on the right-hand side of Eq. (3.17) is the buoyant term which may be expressed as

$$\left(\frac{\theta_{va} - \theta_{vo}}{\theta}\right) g = (1 - \sigma^2) \left(\frac{\theta_{va} - \theta_{vb}}{\theta}\right) g \tag{3.31}$$

with the aid of (3.28). The model of a solitary updraft column without the compensating current corresponds to the case $\sigma \to 0$. It is obvious that the compensating motion tends to reduce the buoyant force acting upon the inner updraft.

4. Kinetic energy equation

Multiplying (3.19) by w_a and integrating the resulting equation over the entire mass of the inner column and applying the boundary conditions that $w_a = 0$ at $z = 0$ and $z = z_T$, we obtain

$$\int \frac{\partial k_a}{\partial t} \sigma^2 \rho_o dz = \int \left[g\, w_a \left(\frac{\theta_{va} - \theta_{vo}}{\Theta} \right) - \frac{2}{b\sigma} \tilde{u}_a \left(w_a \tilde{w}_a - K_a \right) \right.$$

$$\left. - \frac{4\upsilon}{b^2\sigma^2} \left(K_a - \tfrac{1}{2} w_a w_b \right) \right] \sigma^2 \rho_o dz, \qquad (4.1)$$

where $K_a = \frac{1}{2} w_a^2$.

With the aid of (3.29), the second term on the right-hand side of (4.1) is expressed by

$$-\int \frac{2K_a}{b\sigma} \left| \tilde{u}_a \right| \begin{cases} \dfrac{1 + \sigma^2}{1 - \sigma^2} & \text{if } \tilde{u}_a < 0 \\ 1 & \text{if } \tilde{u}_a > 0 \end{cases} \sigma^2 \rho_o dz. \qquad (4.2)$$

Since the term (4.2) is negative regardless of the sign of $\tilde{u}_a$, the actions of both entrainment and detrainment contribute to the dissipation of kinetic energy.

With the aid of (3.27), the third term on the right-hand side of (4.1) is expressed by

$$- \int \frac{4\nu}{b^2\sigma^2} \frac{1}{1 - \sigma^2} K_a \sigma^2 \rho_o dz \ . \tag{4.3}$$

The term (4.3) is negative and has a dissipation effect.

The first term on the right-hand side of (4.1) can be rewritten as

$$\int g w_a \left(\frac{\theta_{va} - \theta_{vb}}{\Theta} \right) (1 - \sigma^2) \sigma^2 \rho_o dz \tag{4.4}$$

with the aid of (3.31). This integral can be either negative or positive depending on the value of the product $w_a(\theta_{va} - \theta_{vb})$. When the ascending air in the inner column is warmer than the air in the outer column, the product is positive and vice versa. Therefore, we shall call the integral (4.4) as the energy producing term.

The total kinetic energy of the outer column K_b is expressed by

$$K_b \equiv \frac{1}{2} w_b^2 = \left(\frac{\sigma^2}{1 - \sigma^2} \right)^2 K_a \tag{4.5}$$

with the aid of (3.27).

Thus, the total kinetic energy K of the whole system can be shown as

$$K \equiv \sigma^2 K_a + (1 - \sigma^2) K_b = \left(\frac{\sigma^2}{1 - \sigma^2} \right) K_a \ . \tag{4.6}$$

By substituting (4.2) $\sim$ (4.4) into (4.1) and using (4.6), we obtain

$$\int \frac{\partial K}{\partial t} \rho_o dz = \int \left\{ g w_a \left(\frac{\theta_{va} - \theta_{vb}}{\Theta} \right) \sigma^2 - \frac{2K}{b\sigma} |\tilde{u}_a| \begin{cases} \dfrac{1+\sigma^2}{1-\sigma^2} & \text{if } \tilde{u}_a < 0 \\ 1 & \text{if } \tilde{u}_a > 0 \end{cases} - \frac{4\nu K}{b^2\sigma^2(1-\sigma^2)} \right\} \rho_o \, dz . \tag{4.7}$$

5. Perturbation analysis

In this section, we shall present the results of analysis based on linearized equations to illustrate essential physical characteristics of the model.

We assume that perturbation quantities are so small in magnitude that the nonlinear terms in the basic equations can be ignored. Thus, we obtain the following set of linear equations.

$$\frac{\partial w_a}{\partial t} = g\left(\frac{\theta_a - \theta_o}{\Theta}\right) - \frac{2\nu}{b^2\sigma^2} (w_a - w_b) , \tag{5.1}$$

$$\sigma^2 w_a + (1 - \sigma^2) w_b = 0, \tag{5.2}$$

$$\frac{\partial \theta_a}{\partial t} = - S_a w_a - \frac{2\nu}{b^2 \sigma^2} (\theta_a - \theta_b) , \tag{5.3}$$

$$\frac{\partial \theta_b}{\partial t} = - S_b w_b - \frac{2\nu}{b^2 (1 - \sigma^2)} (\theta_b - \theta_a) , \tag{5.4}$$

$$\theta_o = \sigma^2 \theta_a + (1 - \sigma^2) \theta_b . \tag{5.5}$$

Eq. (5.1) was derived from (3.19). Eq. (5.2) is identical to (3.27). Eqs. (5.3) and (5.4) were derived from (3.20) and (3.24) respectively. Eq. (5.5) is identical to (3.28) except that averaging is taken for θ instead of θ_v . In these equations, S_a and S_b stand for the static stabilities in the inner and outer columns in which the moist and dry adiabatic processes are assumed respectively. Therefore, we express

$$S_a \equiv \frac{\partial \theta_e}{\partial z} \doteq \frac{\theta}{T} \left[\frac{\partial T}{\partial z} - \left(\frac{\partial T}{\partial z} \right)_s \right] ,$$

$$S_b \equiv \frac{\partial \theta}{\partial z} = \frac{\theta}{T} \left[\frac{\partial T}{\partial z} - \left(\frac{\partial T}{\partial z} \right)_a \right] , \tag{5.6}$$

where θ and θ_e are the potential temperature and the equivalent potential temperature of the basic field, respectively. Also, $-(\partial T/\partial z)_s$ and $-(\partial T/\partial z)_a$ are respectively the saturation-adiabatic and dry-adiabatic lapse rates; and $-(\partial T/\partial z)$ is the temperature lapse rate of the basic field.

Applying (5.5) to (5.1), and eliminating w_b from (5.1) by using (5.2), we obtain

$$\frac{\partial w_a}{\partial t} = g(1 - \sigma^2) \frac{(\theta_a - \theta_b)}{\Theta} - \frac{2\nu w_a}{b^2\sigma^2(1 - \sigma^2)} . \tag{5.7}$$

By subtracting (5.4) from (5.3) and eliminating w_b with the aid of (5.2), we get

$$\frac{\partial}{\partial t} (\theta_a - \theta_b) = S_b \left(\delta - \frac{\sigma^2}{1 - \sigma^2} \right) w_a - \frac{2\nu (\theta_a - \theta_b)}{b^2\sigma^2 (1 - \sigma^2)} \tag{5.8}$$

where

$$\delta = - S_a/S_b . \tag{5.9}$$

If we eliminate $(\theta_a - \theta_b)$ between (5.7) and (5.8), we obtain the following equation for w_a,

$$\left\{ \left[\frac{\partial}{\partial t} + \frac{2\nu}{b^2\sigma^2(1-\sigma^2)} \right]^2 + \frac{gS_b}{\Theta} \left[\sigma^2 - (1-\sigma^2)\,\delta \right] \right\} w_a = 0 \,.$$

Assuming that w_a is proportional to $e^{\eta t}$, we get the following frequency equation

$$\frac{\eta}{\eta_g} = -\frac{\mu}{\sigma^2(1-\sigma^2)} \pm \sqrt{(1-\sigma^2)\,\delta - \sigma^2} \,, \tag{5.10}$$

where $\eta_g = \sqrt{g\, S_b / \Theta}$, the frequency of Brunt-Väisälä oscillation and

$$\mu = \frac{2\nu}{b^2 \eta_g} \,.$$

Let us select the following values for the parameters:

$$\begin{aligned} g &\simeq 10^3 \text{ cm sec}^{-2} \\ S_b/\Theta &\simeq 10^{-7} \text{ cm}^{-1} \\ \nu &\simeq 5 \times 10^4 \text{ cm}^2 \text{ sec}^{-1} \\ b &\simeq 10^5 \sim 10^6 \text{ cm} \,. \end{aligned} \tag{5.11}$$

Then we obtain

$$\eta_g = 10^{-2} \text{ sec}^{-1}$$

$$\mu \approx 10^{-3} \sim 10^{-5}.$$

In the absence of dissipation, it is shown from (5.10) that the perturbations grow exponentially if

$$\delta > \frac{\sigma^2}{1 - \sigma^2} \geq 0 \tag{5.12}$$

or with the definition of δ given by (5.9) and (5.6), (5.12) can be written as

$$\frac{\partial T}{\partial z} < \left(\frac{\partial T}{\partial z}\right)_s (1 - \sigma^2) + \left(\frac{\partial T}{\partial z}\right)_a \sigma^2 . \tag{5.13}$$

The case of $\sigma \to 0$ implies infinitely narrow jets of rising air. In this case, (5.13) reduces to the classical criterion

$$\frac{\partial T}{\partial z} < \left(\frac{\partial T}{\partial z}\right)_s$$

for the onset of convection.

The condition (5.12) implies that the cumulus convection does not occur unless the ratio between the width of the cumulus towers and that of the cloudless intervals is below a certain critical value. This result was first pointed out by J. Bjerknes (1938). Later, Haque (1952) and Lilly (1960) discussed similar conditions in connection with the formation of tropical cyclones.

Fig. 2

With reference to the frequency equation (5.10), Fig. 2 shows the dependence of the growth rate n/n_g of perturbations upon the area density of the updraft σ^2, the coefficient of dissipation μ and the stability ratio δ. In a mean tropical atmosphere, below the 500 mb level, the value of δ ranges from 0.5 to 1. The solid lines show the case of $\delta = 1$ and the dashed lines show the case of $\delta = 0.5$. Four lines in each case show for $\mu = 0$, 10^{-5}, 10^{-4}, and 10^{-3}, except for the dashed line corresponding to $\mu = 10^{-3}$ which is missing in this figure because the magnitude n/n_g is less than 10^{-2}. In general, it is seen that the growth rate curves show two sharp cut-off ends, one at a large value of σ and the other at a small value of σ. As it was discussed that the cut-off at a larger σ is due to the compensating current associated with the updraft and therefore the value of σ for the cut-off depends mainly on the value of δ. On the other hand, the other cut-off at a smaller σ is due to the dissipative effect of turbulent exchanges between the inner and outer columns. Thus, the value of σ for the cut-off depends mainly on the value of μ. It appears that the dependence of the growth rate

on the value of μ is very sensitive. In the nonlinear version of the model, however, the effect of turbulent exchanges does not appear as sensitive as that of the linear case, since the effect of dynamic entrainment usually dominates over the effect of mixing in the nonlinear model. At any rate it is seen that the maximum growth rate appears roughly at $\sigma = 0.1 \sim 0.3$. A similar conclusion has been derived by Kuo (1961).

6. Environmental and initial conditions

In order to obtain numerical solutions of Eqs. (3.19) to (3.27), we choose the following two cases as typical environmental atmospheric conditions.

Case I: The temperature distribution has the lapse rate of $6^{o}C\ km^{-1}$ with $25^{o}C$ at the earth's surface and the distribution of relative humidity has the decreasing rate of 5% per kilometer with 90% at the surface.

Case II: The same as Case I except for the value of relative humidity at the surface being 100% instead of 90%.

In other words, taking z = 0 at the surface, we can write the distributions of temperature T(z) and relative humidity R(z) as follows:

$$T(z) = T(0) - \Gamma z \tag{6.1}$$

$$R(z) = R(0) - \gamma z \tag{6.2}$$

where

$$\left.\begin{aligned} \Gamma &= 6^{o}C\ km^{-1} \\ T(0) &= 25^{o} + 273.16^{o}K \\ \gamma &= .05\ km^{-1} \end{aligned}\right\} \quad \text{For Cases I and II}$$

$$R(0) = .90 \quad \text{For Case I}$$

$$1.00 \quad \text{For Case II.}$$

The distributions of pressure p, potential temperature θ, saturation-specific humidity q_s and specific humidity q can be computed from the distributions of T and R as follows:

$$p(z) = p(0)\ [T(z)/T(0)]^{\frac{g}{R\Gamma}}$$

$$\theta(z) = T(0)\ [p(z)/p(0)]^{\kappa}$$

$$q_s(z) = [3.8 \exp \left\{ \frac{a_1\ (T - 273.16)}{T - a_2} \right\}]\ /p$$

$$q(z) = R\ q_s$$

where $a_1 = 17.27$ and $a_2 = 35.86$ according to Teten's formula. The thermal stratification described by the present temperature distribution is conditionally unstable below the level of about 5.5 km and stable above that level.

The top of the air column is assumed to be at z = 15 km where the vertical motions vanish. The radius of the whole system, b, is assumed to be 5 km and many numerical experiments were performed by varying the value of σ .

The excess temperature ΔT_a in the layer below 2 km in the inner column is assumed initially to be in the following form

$$\Delta T_a = \Delta T^* \left(\frac{z}{z^*} \right) \left(2 - \frac{z}{z^*} \right)$$

which is represented by a parabola having the maximum ΔT^* (= $1^{\circ}K$) at $z = z^*$ (= 1 km). It is assumed that this heated layer is initially saturated with water vapor.

In order to solve Eqs. (3.19) to (3.27) numerically as an initial value problem, finite-difference equations must be written for the partial differential equations with respect to time t and height z . The uncentered difference scheme which was used successfully by Asai (1962) is applied here. In order to save space, we shall omit the finite-difference equations. A time step Δt of 5 seconds and a height increment Δz of 100 meters are used. All computations were performed up to the period of one hour which corresponds to 720 time steps.

7. Results

We are going to discuss the results of two cases.

Case I: Fig. 3(a) and (b) show the time sections of the distributions of the vertical velocity w_a and the potential temperature deviation $\Delta\theta_a$ from the environmental value given by (6.3). These results are for the

---

Fig. 3(a) and (b)

---

inner column and $\sigma = 0.2$. The ordinate shows the height in kilometers and the abscissa denotes the time in minutes. The shaded area in Fig. 3(a) shows the domain of the cloud in which the air is saturated with water vapor. The top of the cloud ascends with the speed of about 3.4 m/sec until the cloud top reaches the 4-km level. The thickness of the cloud was initially 2 km and it was preserved during the period of 10 minutes from the start. After this period, the increase in the height of the cloud top almost stops and the thickness of the cloud reduces. After about 16 minutes, the cloud disappears completely and then there remains a stable oscillation with a period of about 10 minutes which is found equal to the period of Brunt-Väisälä oscillation for the present thermal stratification. Note that there is a phase lag of a quarter of the period between the vertical motion and the temperature deviation patterns as seen from Fig. 3(a) and (b) by comparison.

Although these results are based upon the particular example of $\sigma = 0.2$, similar results were obtained for other runs with different values of σ. Also, it is worthwhile to point out that the results of computation without the compensating downward motion in the outer column are similar to those with the compensating downward motion. It should be borne in mind, however, that the latter finding does not result from Case II. At any rate, it is obvious that no tall cumulus clouds ever form in Case I.

Case II: Here we will compare the results of two different experiments. The same initial and environmental conditions are used in both experiments, but one experiment does not include the effect of the compensating current and therefore the calculation reduces to that of a single column.

Fig. 4(a) and (b)

(c) and (d)

Fig. 4(a) and (b) show the time sections of the distributions of the vertical velocity and the potential temperature deviation from the environmental value.

Fig. 4(c) and (d) show the specific humidity deviation from the environmental value and the liquid water content, respectively. These results are for the inner column and $\sigma = 0.2$. The results of Exp. I (with compensating downward motions in the outer column) are indicated by solid

lines and those of Exp. II (without the compensating downward motions) by dashed lines.

For both experiments, the upward motions and temperature deviations increase with respect to time, and the cloud tops reach a height of 8 km after about 20 minutes. Beyond this growing period, the structure of the cloud in Exp. II becomes more or less stationary. However, the structure of the cloud in Exp. I shows a different evolution. After about 20 minutes from the start, the downward motion develops first at the lowest layer of the inner column and then propagates to the upper portion, while the height of the updraft maximum and the cloud top continue to rise, despite the fact that a cooling developed above a height of 6 km. After about 30 minutes from the start, the cooling at the 8-km height intensifies sufficiently and the downward motion develops in the core. This stage appears to be the end of the cloud development and, from this time on, the cloud undergoes a stable oscillatory regime.

Differences in the evolution of the clouds in the two experiments are very interesting. Without the effect of the compensating downward motion, the structure of the single column updraft can reach a steady state. Apparently, the compensating downward motion acts as a "break" which prevents the maintenance of a tall cumulus cloud. Another point of interest is that the cloud top in Case II was able to penetrate into the upper stable layer and reach to the 8 km level, whereas in Case I the cloud top reached only the 4 km level. However, the height of the cloud base could not be maintained in Exp. II. It is apparent, therefore, that a constant supply of

moisture into the lower layer of the updraft is necessary to produce and maintain a tall cumulus cloud.

We now discuss a dependence of the cloud development on the parameter σ, the ratio of the radius of the inner column to that of the outer column. A number of computations were made for Case II, varying the value of σ. The following energy integrals are computed at each time step:

i. The total kinetic energy E_a per unit horizontal area for the inner column defined by

$$E_a = \int K_a \rho_o dz .$$

ii. The total kinetic energy E for unit horizontal area for the whole system defined by

$$E = \frac{\sigma^2}{1 - \sigma^2} E_a$$

with reference to (4.6).

iii. The vertical heat transport H_T for the whole system integrated during the computation period considered here (40 minutes).

$$H_T = \iint \sigma^2 \, gw_a \left(\frac{\theta_{va} - \theta_{vb}}{\Theta} \right) \rho_o \, dz \, dt .$$

Fig. 5

In Fig. 5, the ordinate shows the scale of energy, the upper abscissa shows the parameter σ and the lower one shows σ^2 . The broken line shows the maximum kinetic energy E_{max} during a period of 40 minutes. The maximum of the curve appears at $\sigma^2 = 0.1$ (or $\sigma = 0.32$). The solid line shows the total vertical heat transport integrated over the computation period. Again the maximum appears at $\sigma^2 = 0.1$. Thus we conclude that the most active cloud system appears for a particular value of the ratio of the upward motion area to the entire area, namely $\sigma^2 = 0.1$.

The thin solid line denoted by Ea_{max} shows the maximum kinetic energy for only the inner area. The maximum of the curve appears around $\sigma^2 = 0.01$. This implies that the intensity of the updraft increases as the domain of the updraft decreases up to the point that the amount of energy dissipation due to turbulence finally exceeds the conversion of potential energy into kinetic energy. It is seen that the most efficient upward heat transport does not necessarily occur at the scale of the most intense cloud for which E_a is maximum.

8. Conclusions

The study was made to assess the effect of compensating downward motions upon the development of cumulus clouds. It is an extension of the so-called "slice method," given by Bjerknes (1938). In order to allow for the compensating downward motions associated with the updraft, the model

consists of two circular concentric air columns. The governing equations of motion in both regions were solved numerically, treated as an initial value problem. The thermal stratification of the environmental temperature distribution used in this study is conditionally unstable below the level of about 5.5 km and stable above that level. The following conclusions are derived from the results of the present calculations:

(1) When the environmental field is relatively dry and without a steady source of moisture, tall clouds never develop. When a cloud forms, it ascends up to the top of the unstable layer and then disappears. There remains a stable oscillation with a period of about 10 minutes which is equal to the period of the Brunt-V$\ddot{a}$is$\ddot{a}$l$\ddot{a}$ oscillation. Effects of the compensating downward motion are not so important in this case.

(2) When the environmental field is relatively moist, a tall cloud can develop and may be maintained if we disregard the influence of compensating downward motions. This result seems to give a basis for the consideration of steady-states for the single-column cumulus model. However, this conclusion is no more valid if we take into account the compensating downward motions.

(3) Under the influence of compensating downward motions, a tall cloud can develop, but the lifetime of the cloud lasts only about 40 minutes without a steady source of moisture. It is an interesting conjecture that there are no steady-state solutions to the governing equations in this case.

(4) The development of clouds depends on, among other things, the parameter σ^2 - the area density of the cloud - which is the ratio of the area of the cloud to that of the whole system including the cloudless area associated with the cloud. It was found that the most efficient vertical heat transfer occurs at $\sigma^2 = 0.1$. This suggests that the most active cloud system appears when the cloud towers occupy the 10 percent of a given area. From a photogrammetric study of the distribution of cumulus clouds in a hurricane by Malkus, Ronne and Chaffee (1961), they found that the cloud coverage in the central part of the hurricane is around several percent. This may be interpreted to mean that cumulus clouds are formed in hurricanes to carry heat upwards with the most efficient rate.

In this study, the condition at the wall of the outer boundary is assumed so that there is no flow through the boundary. In reality, large-scale synoptic conditions influence the development of cumulus clouds. The influence of environmental motions can be taken into account in this model by allowing flow through the outer boundary of the system. This will be discussed in a separate report.

REFERENCES

Asai, T., 1962: Numerical experiment of convection in the model atmosphere. Proceedings of the International Symposium on Numerical Weather Prediction in Tokyo, Nov. 1960, 467-476.

_____, 1965: A numerical study of the air-mass transformation over the Japan Sea in winter. Journal of Meteor. Soc. Japan, Ser II, 43, 1-15.

Austin, J. M., 1948: A note on cumulus growth in a nonsaturated environment. J. Meteor., 5, 103-107.

Austin, J. M. and A. Fleisher, 1948: A thermodynamic analysis of cumulus convection. J. Meteor., 5, 240-243.

Bjerknes, J., 1938: Saturated-adiabatic ascent of air through dry-adiabatically descending environment. Quart. J. Roy. Meteor. Soc., 64, 325-330.

Bunker, A. F., 1953: Diffusion, entrainment and frictional drag associated with non-saturated, buoyant air parcels rising through a turbulent air mass. J. Meteor., 10, 212-218.

Byers, H. R. and R. R. Braham, 1949: The thunderstorm. U. S. Dept. of Commerce, Washington, D. C., 287 pp.

Haltiner, G. J., 1959: On the theory of convective currents. Tellus, 11, 4-15.

Haque, S. M. A., 1952: The initiation of cyclonic circulation in a vertically unstable stagnant air mass. Quart. J. Roy. Meteor. Soc., 78, 394-406.

Houghton, H. G. and H. E. Cramer, 1951: A theory of entrainment in convective currents. J. Meteor., 8, 95-102.

Kuo, H. L., 1961: Convection in conditionally unstable atmosphere. Tellus, 13, 441-459.

Levine, J., 1959: Spherical vortex theory of bubble-like motion in cumulus clouds. J. Meteor., 16, 653-662.

Lilly, D. K., 1960: On the theory of disturbances in a conditionally unstable atmosphere. Monthly Weather Review, 88, 1-17.

Malkus, J. S., C. Ronne and M. Chaffee, 1961: Cloud patterns in Hurricane Daisy, 1958. Tellus, 13, 8-30.

Mason, B. J. and R. Emig, 1961: Calculations of the ascent of a saturated buoyant parcel with mixing. Quart J. Roy. Meteor. Soc., 87, 212-222.

Morton, B. R., G. I. Taylor and J. S. Turner, 1956: Turbulent gravitational convection from maintained and instantaneous sources. Proc. Roy. Soc. A, 234, 1-23.

Richardson, L. F., 1926: Atmospheric diffusion shown on a distance-neighbor graph. Proc. Roy. Soc. A, 110, 709-737.

Scorer, R. S. and F. H. Ludlam, 1953: The bubble theory of penetrative convection. Quart. J. Roy. Meteor Soc., 79, 94-103.

Squires, P. and J. S. Turner, 1962: An entraining jet model for cumulonimbus updrafts. Tellus, 14, 422-434.

Stommel, H., 1947: Entrainment of air into a cumulus cloud. J. Meteor, 4, 91-94.

LEGENDS

Fig. 1. The geometrical configuration of the model.

Fig. 2. The dependence of the growth rate η/η_g of perturbations upon the area density of the updraft σ^2 . The solid lines show the case of $\delta = 1$ and the dashed lines show the case of $\delta = 0.5$.

Fig. 3. The time sections of the distributions of (a) the vertical velocity w_a , and (b) the potential temperature deviation $\Delta\theta_a$ from the environmental value. The shaded area in figure (a) shows the domain of the cloud. These results are for the inner column and $\sigma = 0.2$.

Fig. 4. The time sections of the distributions of (a) the vertical velocity w_a , (b) the potential temperature deviation $\Delta\theta_a$ from the environmental value, (c) the specific humidity deviation Δq_a from the environmental value, and (d) the liquid water content m_a. These results are for the inner column and $\sigma = 0.2$. The results of Exp. I (with compensating downward motions in the outer column) are indicated by solid lines and those of Exp. II (without the compensating downward motions) by dashed lines.

Fig. 5. The dependence of the vertical heat transport H_T (solid line), the maximum kinetic energy E_{max} (broken line) and the maximum kinetic energy for only the inner column Ea_{max} (thin solid line) upon the area density of the updraft σ^2 .

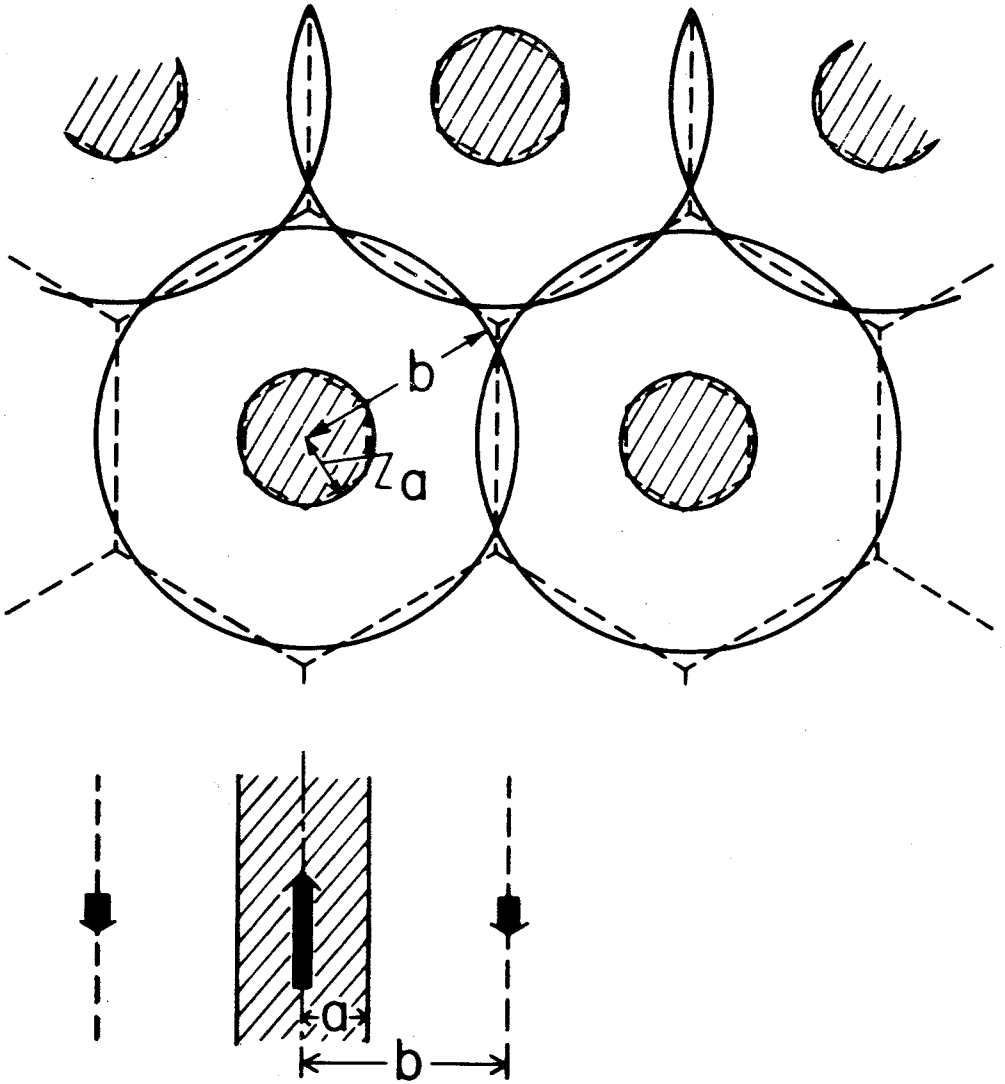

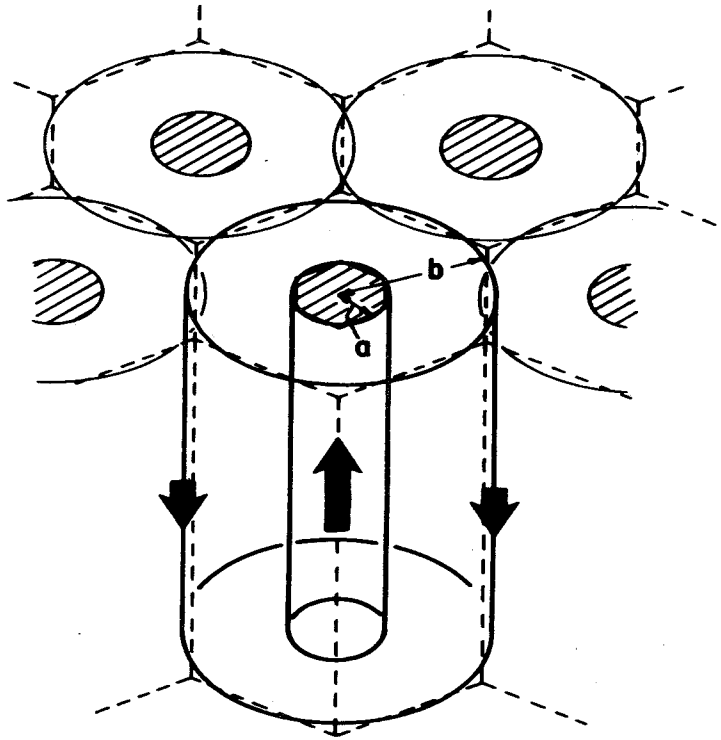

Fig. 1

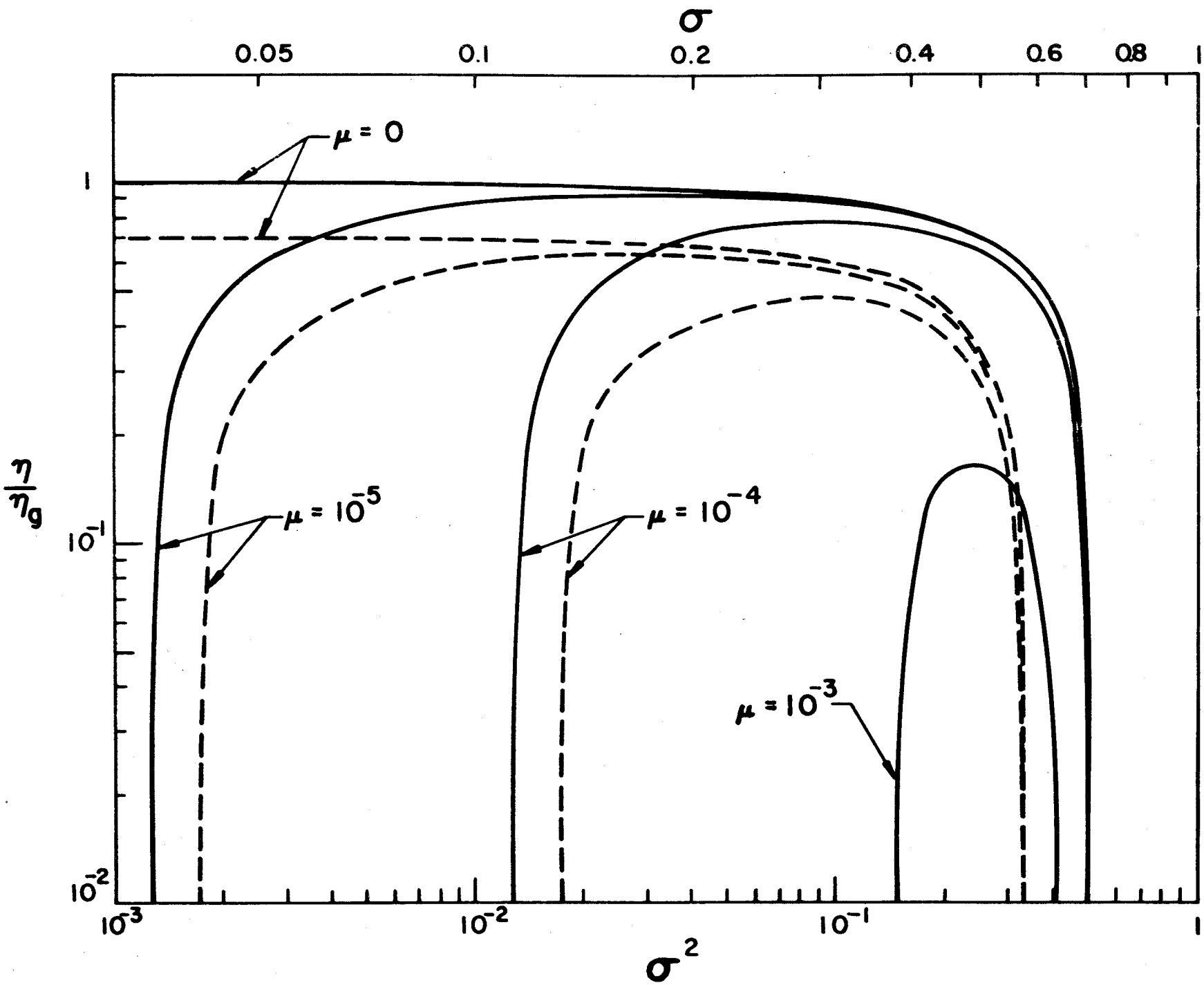
σ
0.05
0.1
0.2
0.4
0.6
0.8
1
μ = 0
μ = 10⁻⁵
μ = 10⁻⁴
μ = 10⁻³
η/η_g
1
10⁻¹
10⁻²
10⁻³
10⁻²
10⁻¹
1
σ²

Fig. 2

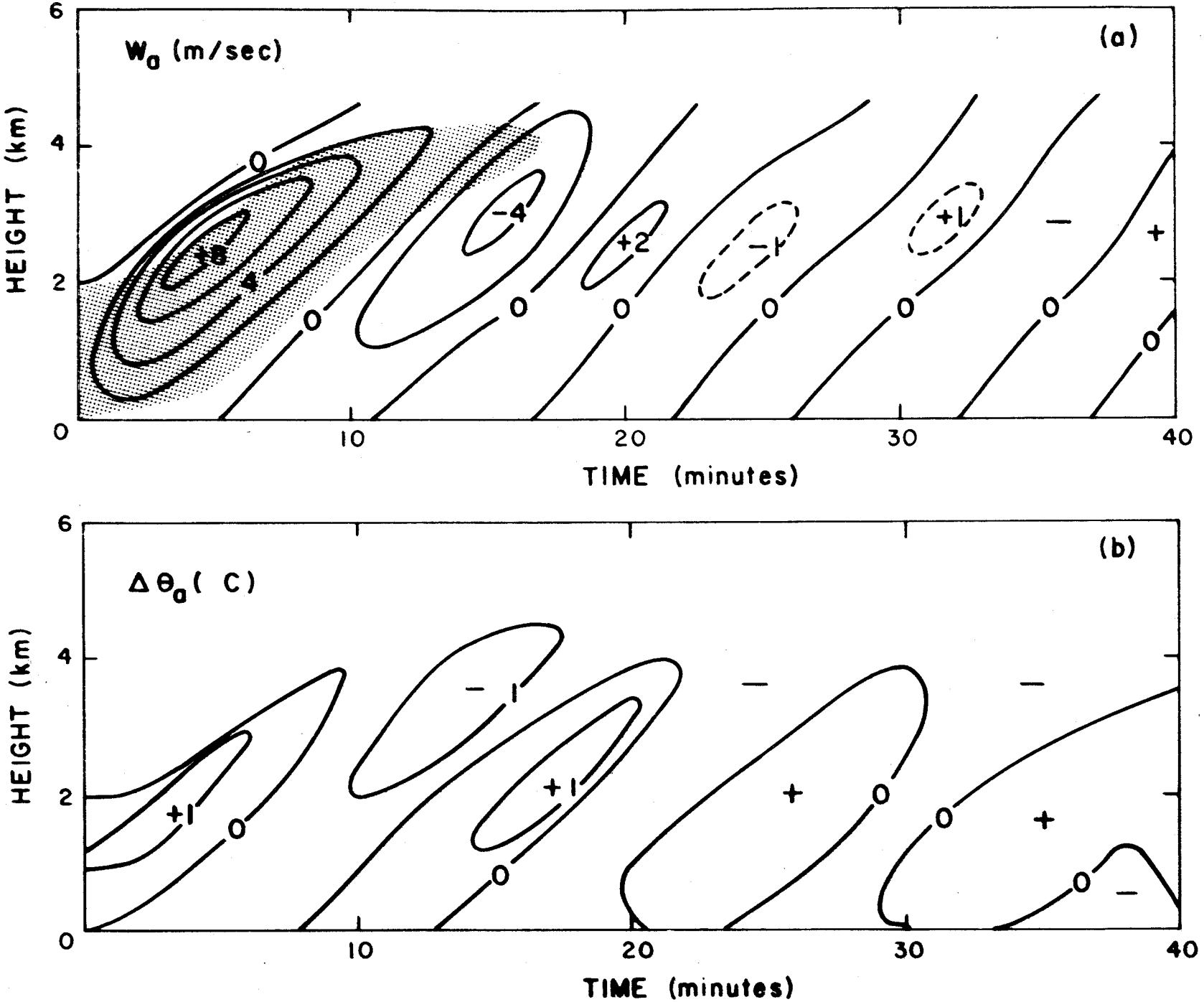
(a)
W_a (m/sec)
HEIGHT (km)
TIME (minutes)
0
2
4
6
10
20
30
40
+8
4
0
-4
+2
-1
+1
(b)
$\Delta\theta_a$ (C)
HEIGHT (km)
TIME (minutes)
+1
-1
+1
+
-

Fig. 3

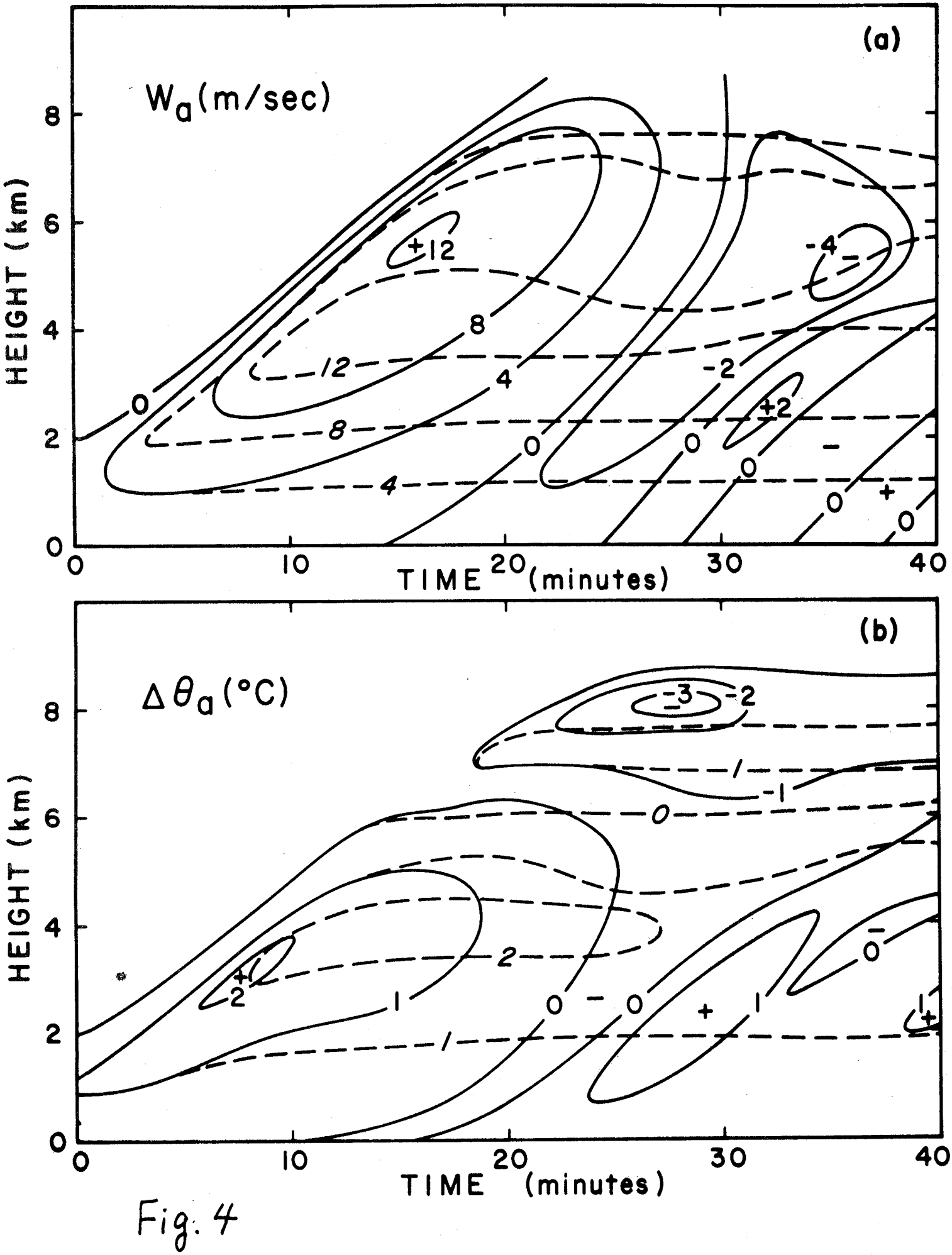
(a)
W_a(m/sec)
HEIGHT (km)
TIME (minutes)
+12
8
12
4
0
8
4
-4
-2
+2
0
0
0
0
+
-
(b)
$\Delta\theta_a$(°C)
HEIGHT (km)
TIME (minutes)
-3
-2
1
-1
0
2
+
2
1
0
0
+
1
0
-
1
+

Fig. 4

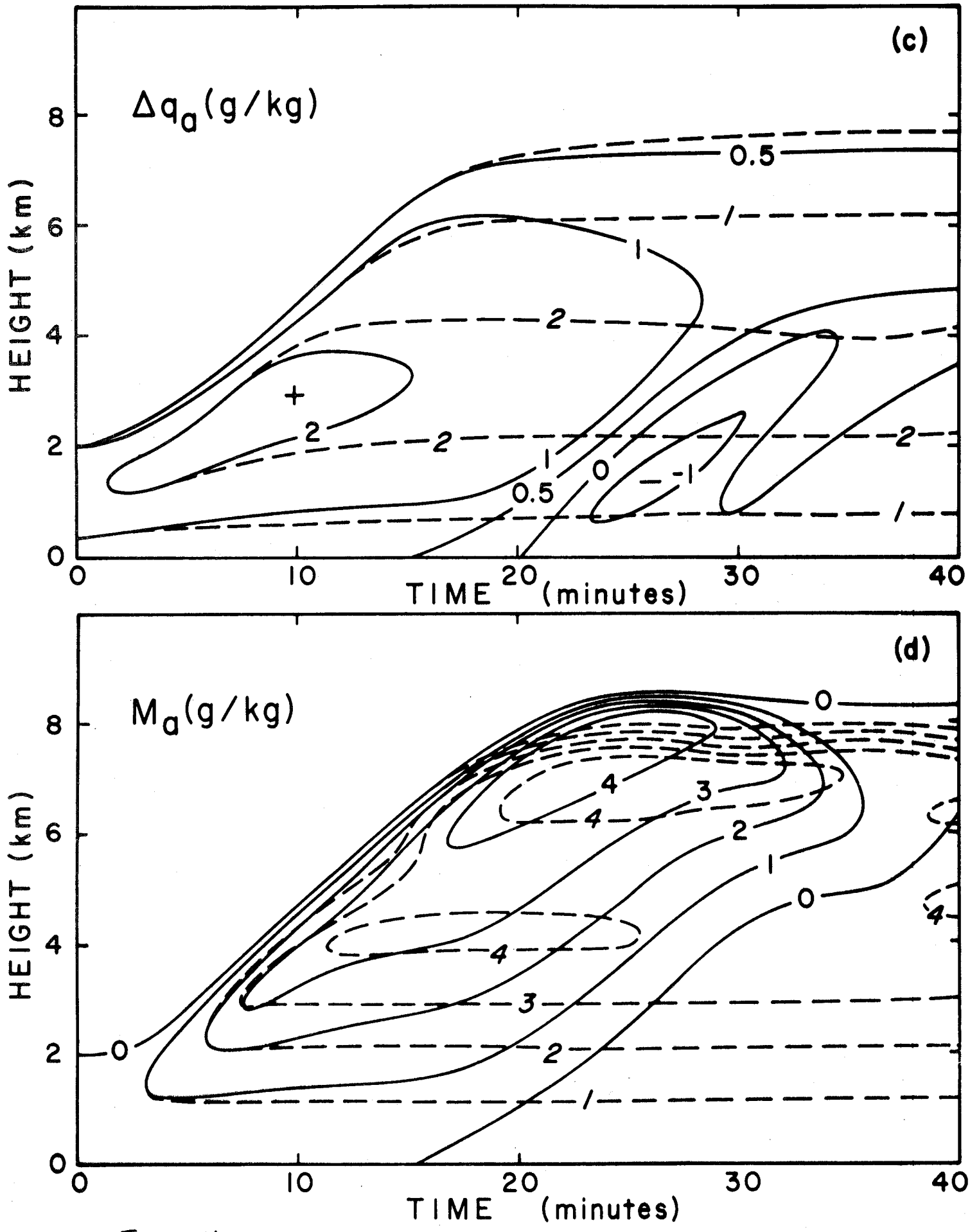
(c)
Δq_a (g/kg)
HEIGHT (km)
TIME (minutes)
0.5
1
2
+
0
-1
(d)
M_a (g/kg)
HEIGHT (km)
TIME (minutes)
0
2
3
4

Fig. 4

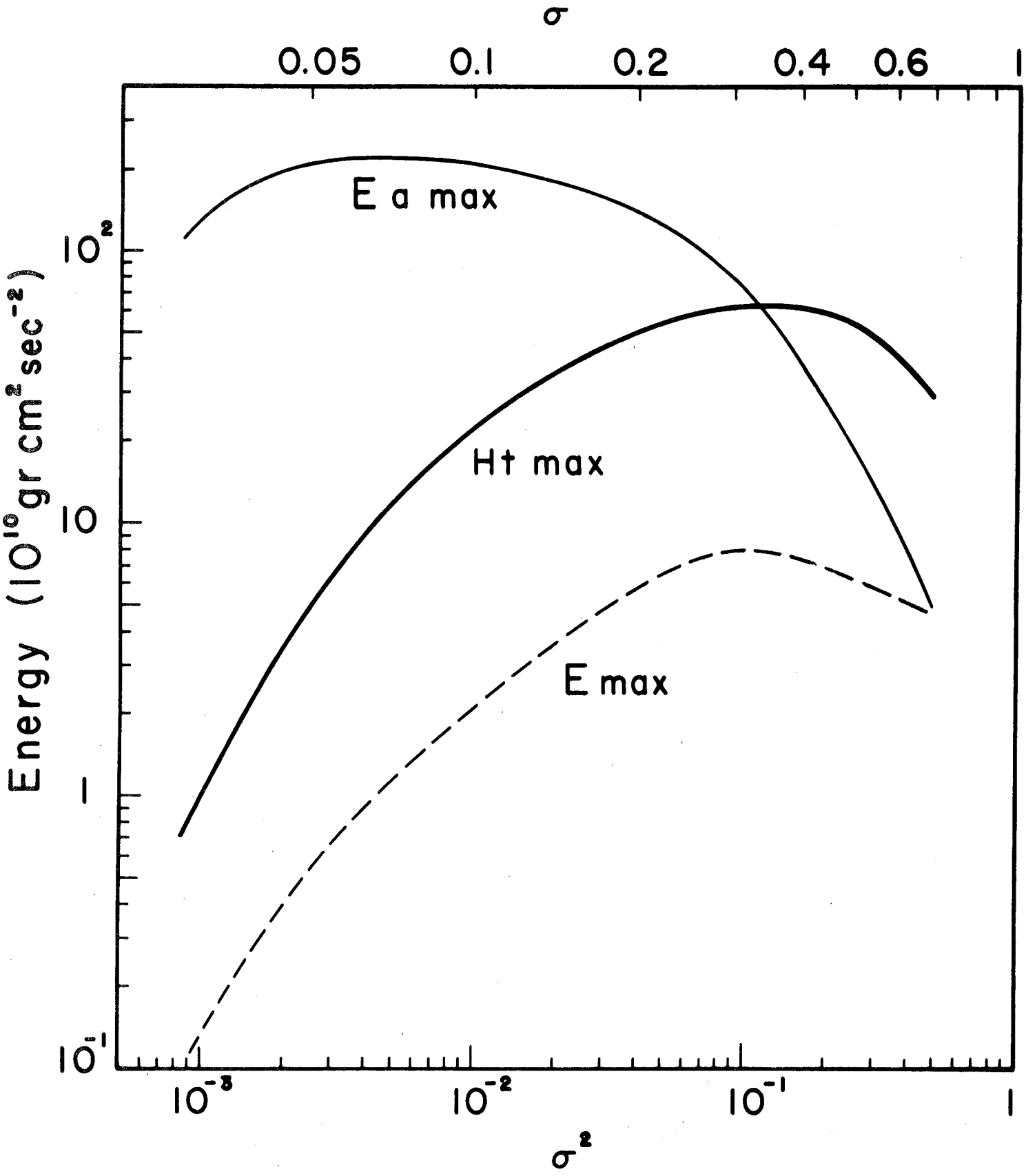
σ
0.05
0.1
0.2
0.4
0.6
1
E a max
Ht max
E max
Energy (10^10 gr cm^2 sec^-2)
10^2
10
1
10^-1
10^-3
10^-2
10^-1
1
σ^2

Fig. 5